Tracking deformation caused by tensile fatigue in quasi-unidirectional glass-fibre composites using a time-lapse correlative study

Anuj Prajapati[1,3], Robert M. Auenhammer[4,5], Stuart Morse[2], Ali Chirazi[3], Daniel Lichau[3], Lars P. Mikkelsen[4], Timothy Burnett[1] and Philip J. Withers[1]

[1] Henry Royce Institute, Department of Materials, The University of Manchester, M13 9PL, United Kingdom

[2] Department of Materials, The University of Manchester, M13 9PL, United Kingdom

[3] Visualization Sciences Group, Thermo Fisher Scientific, Bât E2, 33800 Bordeaux, France

[4] Composite Materials, DTU Wind Energy, Technical University of Denmark, DK-4000, Roskilde, Denmark

[5] Department of Industrial and Materials Science, Chalmers University of Technology, SE-41296, Göteborg, Sweden

Motivation

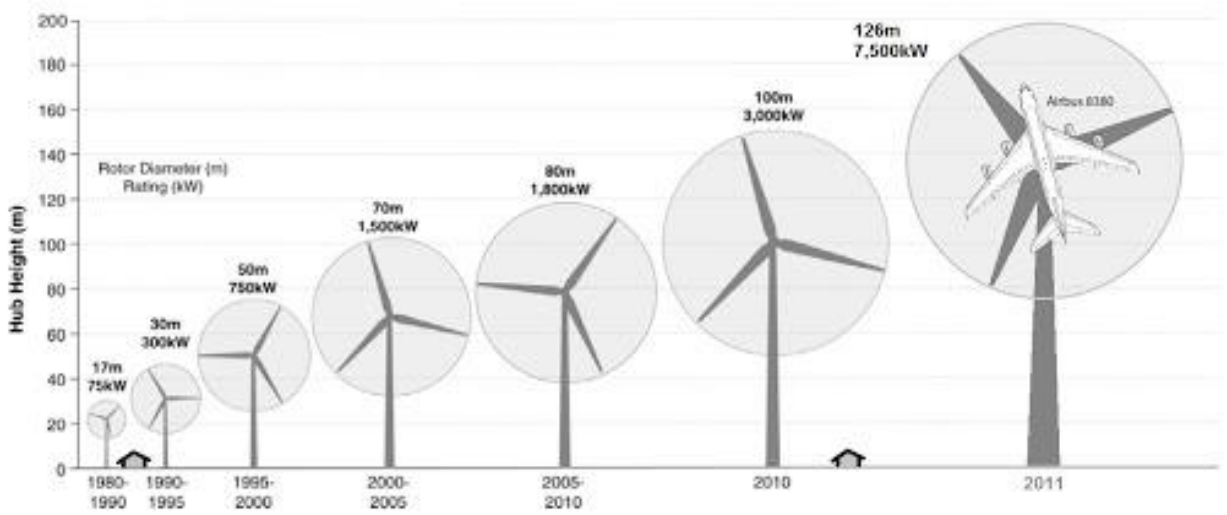

Credit: NZ Wind Energy

- High capital cost Vs better service life and efficiency.

Motivation

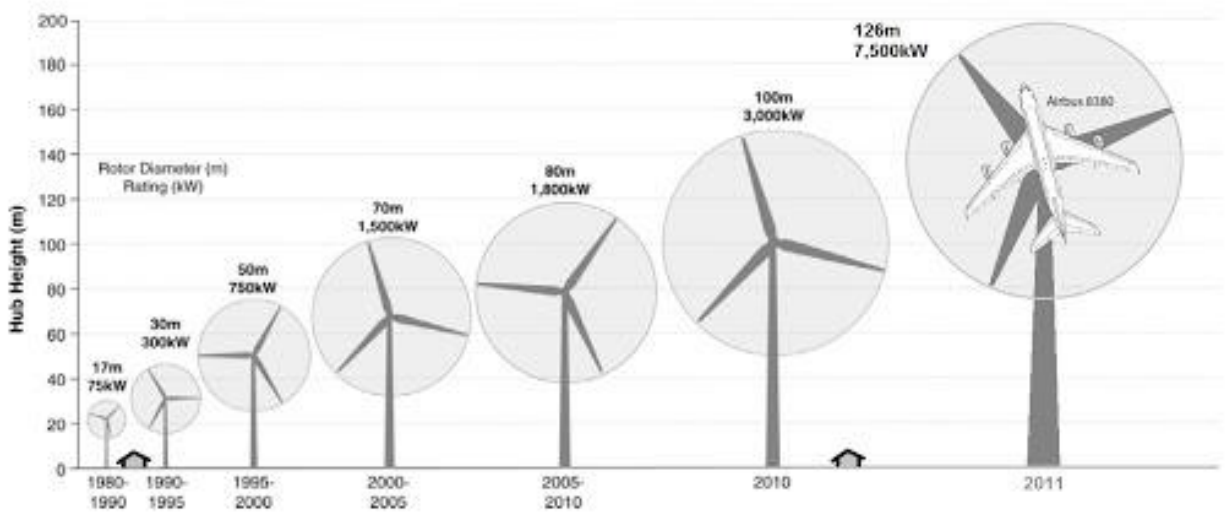

Credit: NZ Wind Energy

- High capital cost Vs better service life and efficiency.
- Bigger blades = higher load carrying capacity.

Motivation

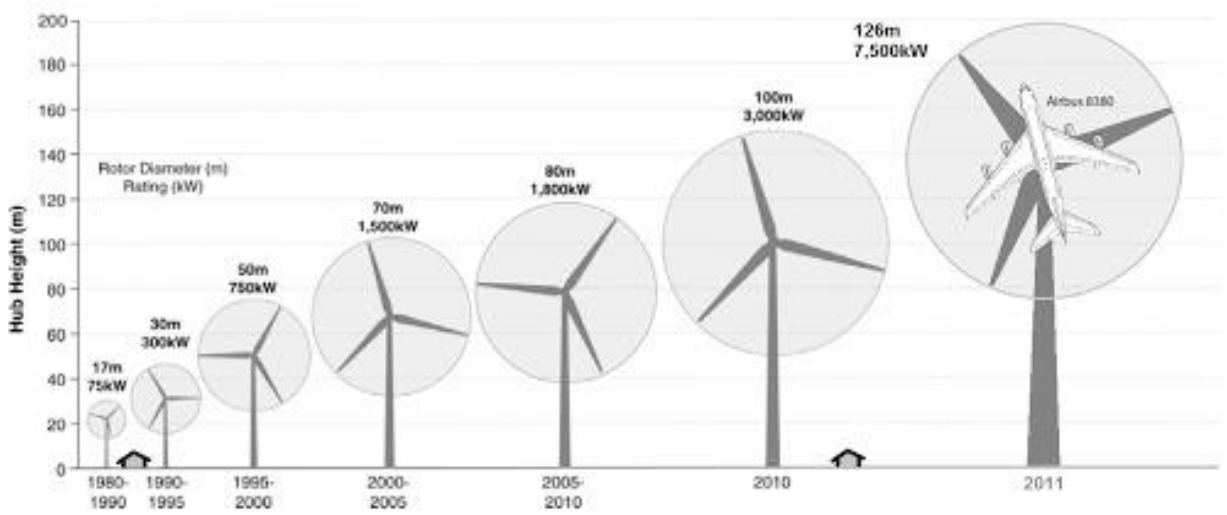

Credit: NZ Wind Energy

- High capital cost Vs better service life and efficiency.
- Bigger blades = higher load carrying capacity.
- Catastrophic failure Vs confidence and adoption rates.

Motivation

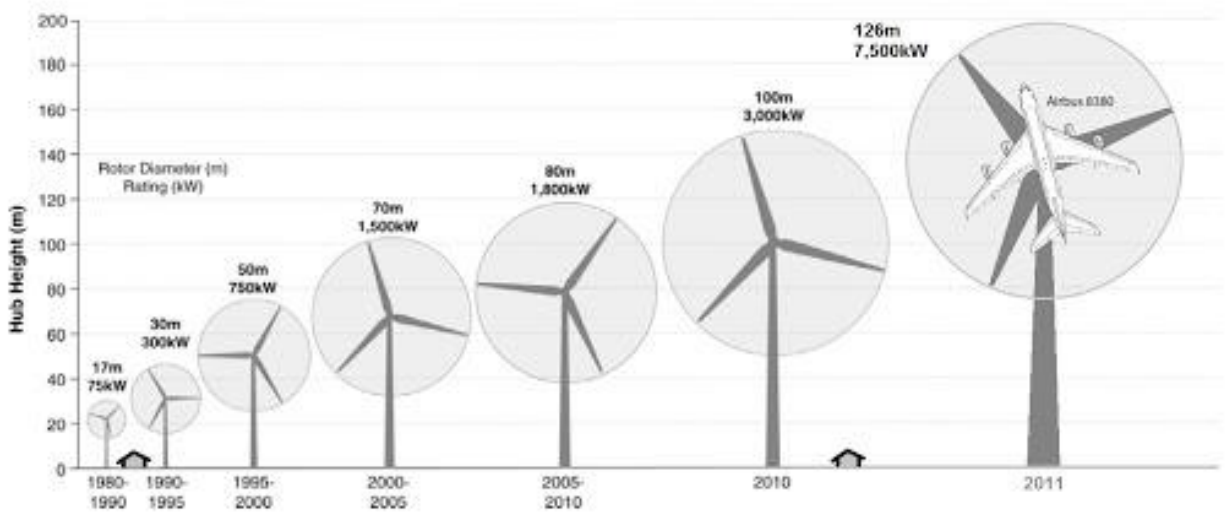

Credit: NZ Wind Energy

- High capital cost Vs better service life and efficiency.
- Bigger blades = higher load carrying capacity.
- Catastrophic failure Vs confidence and adoption rates.
- Optimization of microstructure.

Trinity of materials

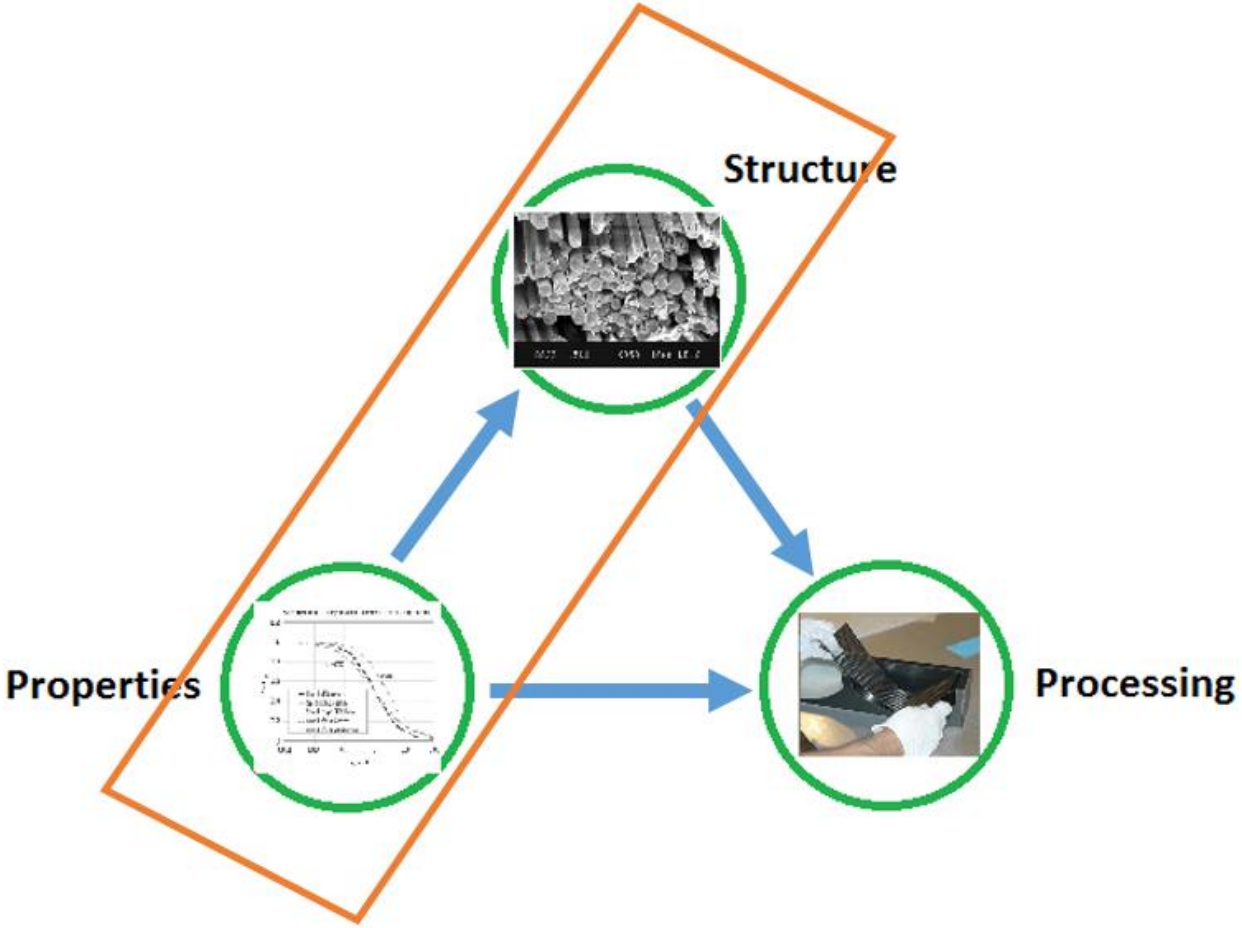

Multiscale dynamic imaging

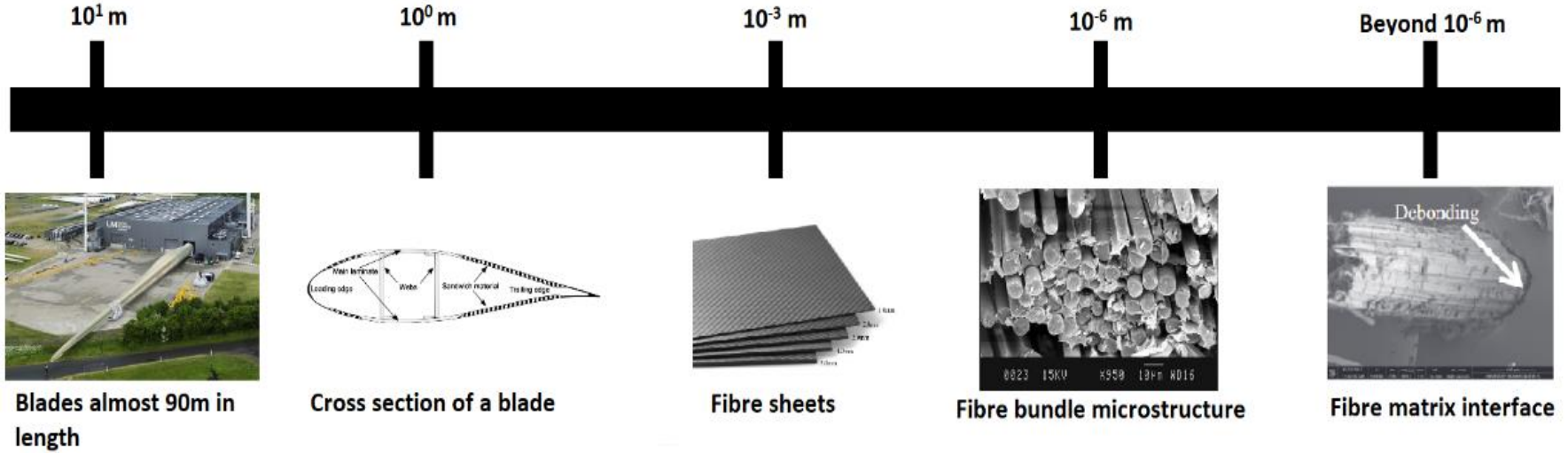

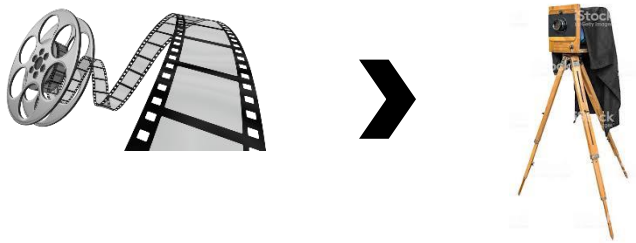

Experiment Design – Workflow

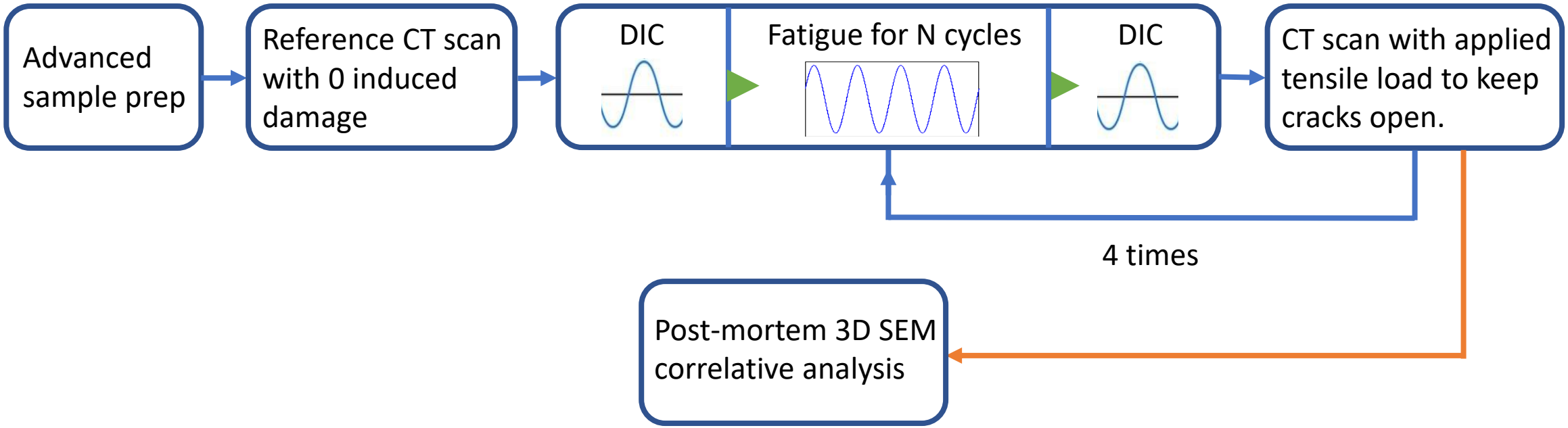

Experiment Design – Sample Prep

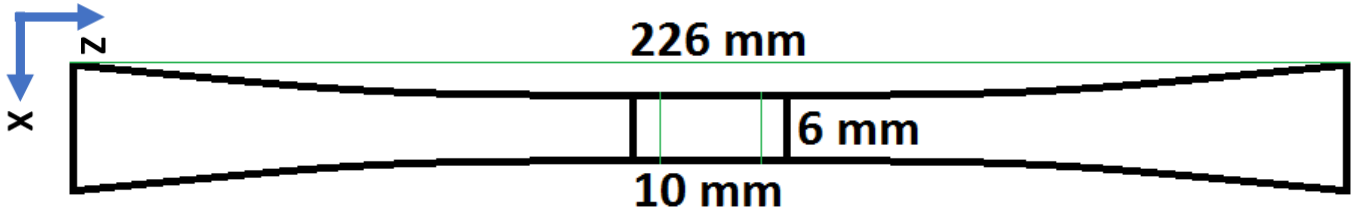

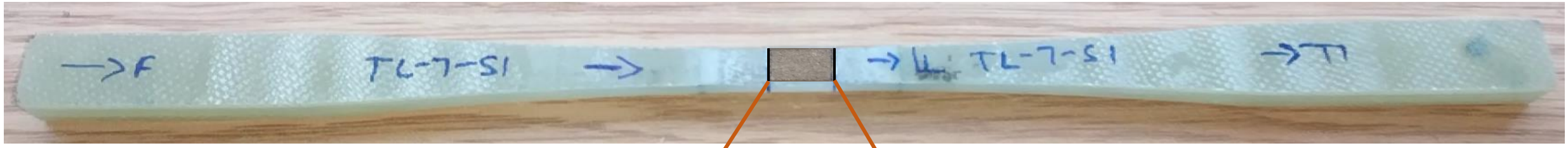

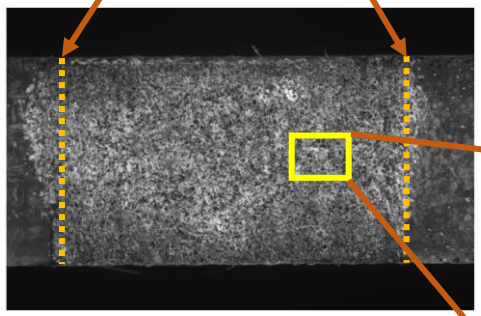

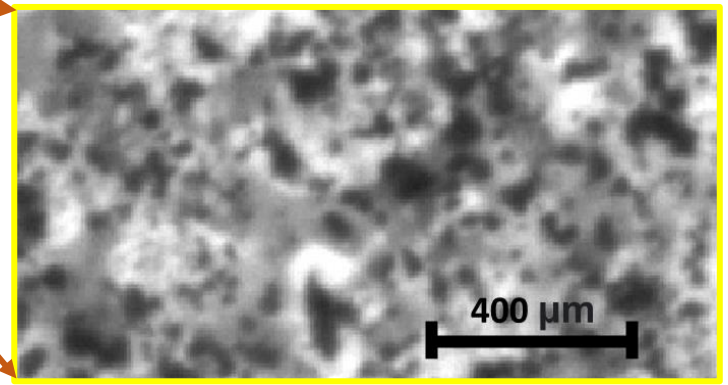

- Tapered tab design.
- UD fibres in direction of arrow, Z direction.
- Backing bundles in X direction.
- Thickness in Y direction.

Experiment Design – CT with tension clamp

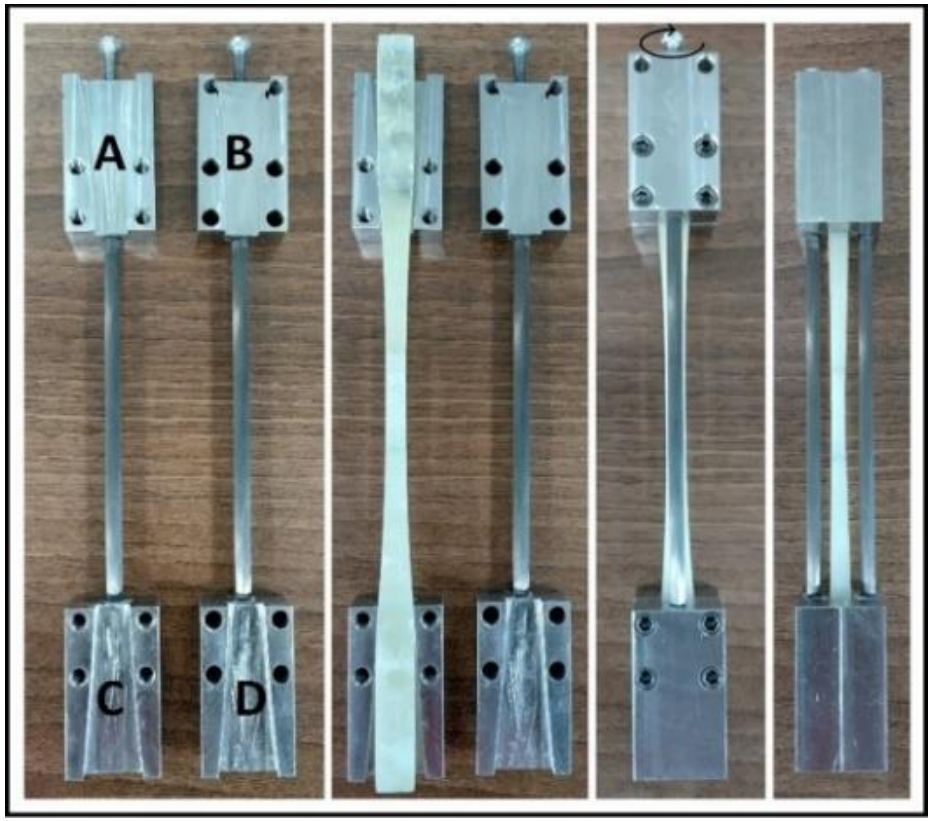

Tension clamp

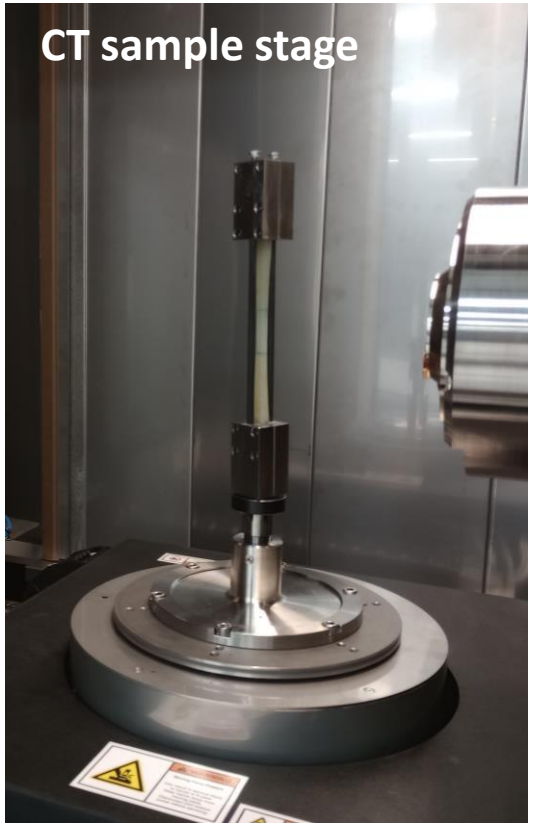

- Steel-plate reinforced carbon rod tips
- Greased rods to move freely and induce no twisting.

Experiment Design – Mechanical testing with DIC

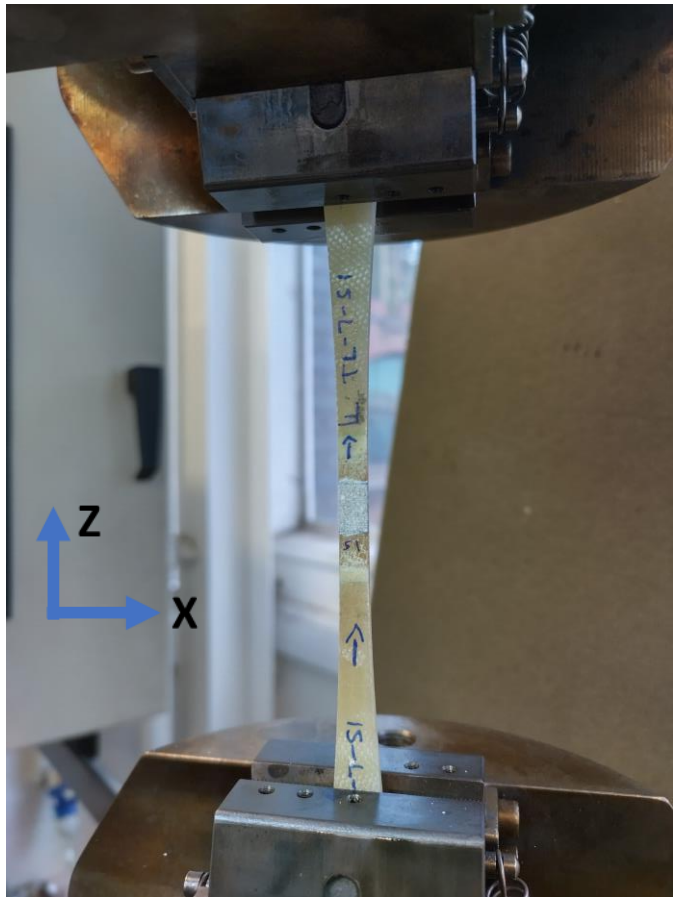

- Single-camera DIC setup.
- DIC acquisition at the start and end of each mechanical fatigue step.
- Dynamic stiffness calculation by a clip-on extensometer.

- 4 Hz, R= 0.1, ε_{max}= 1%, $Load_{max}$= 10kN

Stiffness degradation

- Two-stage stiffness degradation

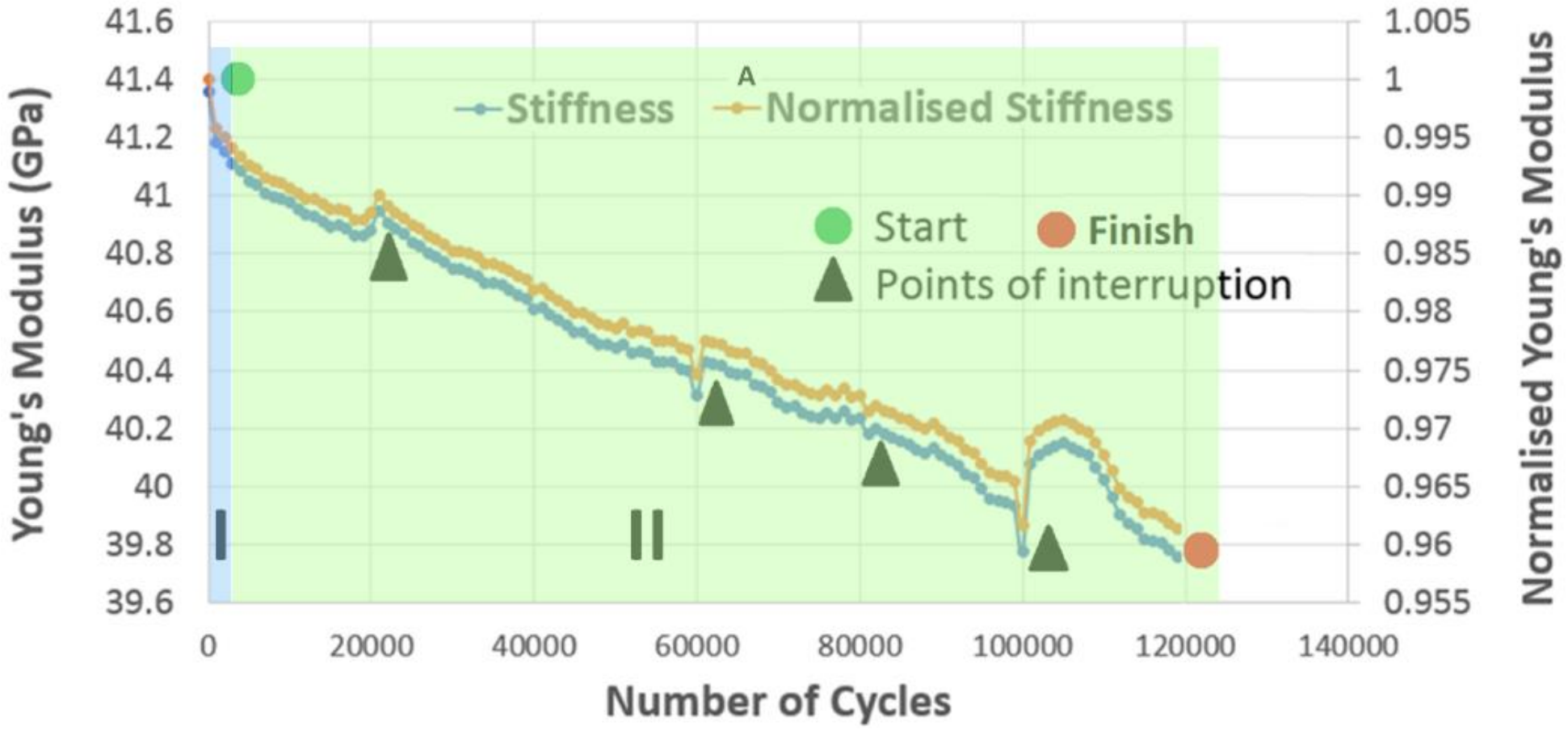

DIC Calculation – Time-lapse

- 31 pixels subset size.
- Strain relative to 0-load reference image.
- Pixel size: 6.53 µm

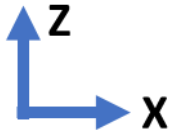

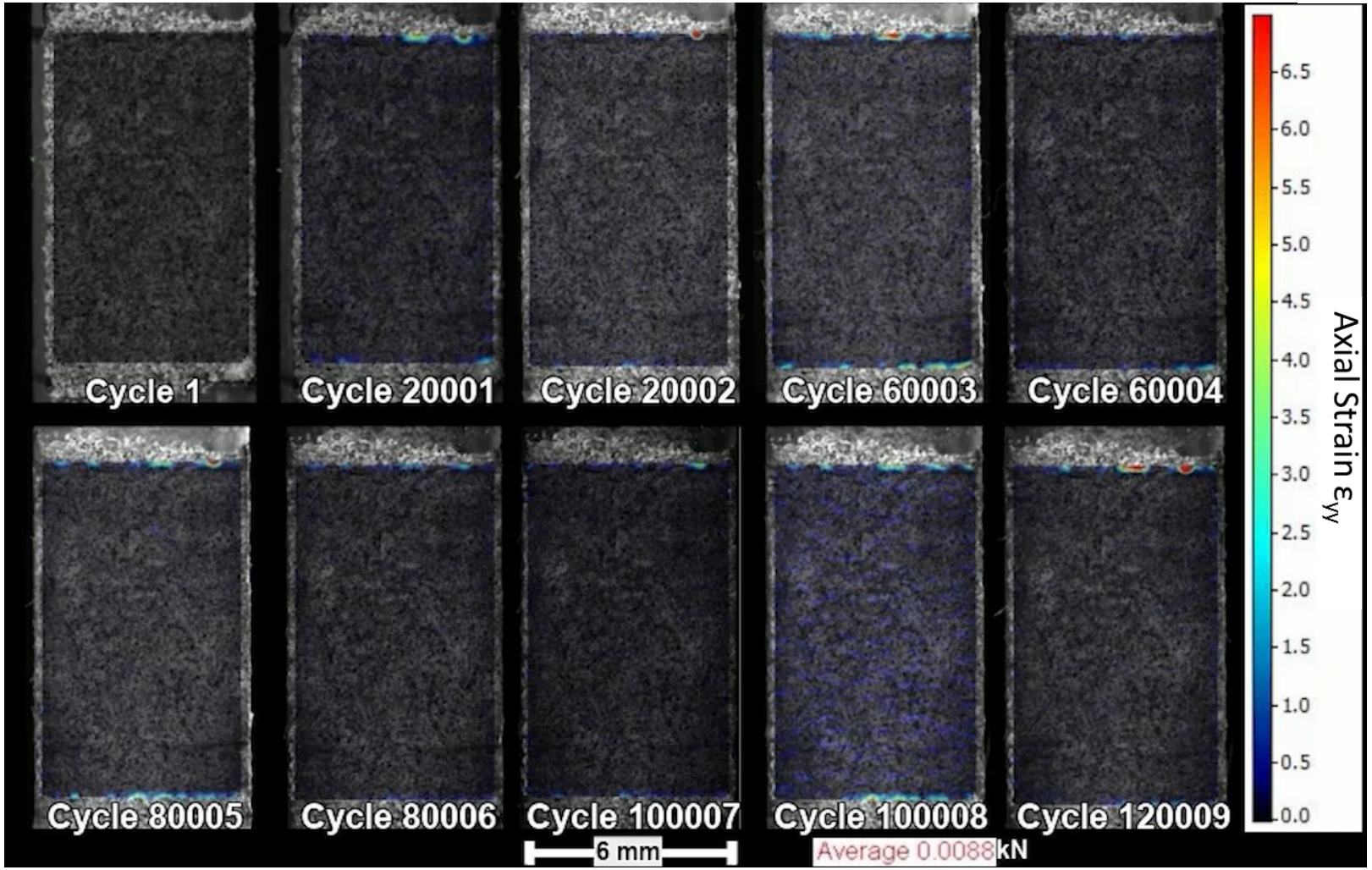

DIC hotspots in CT

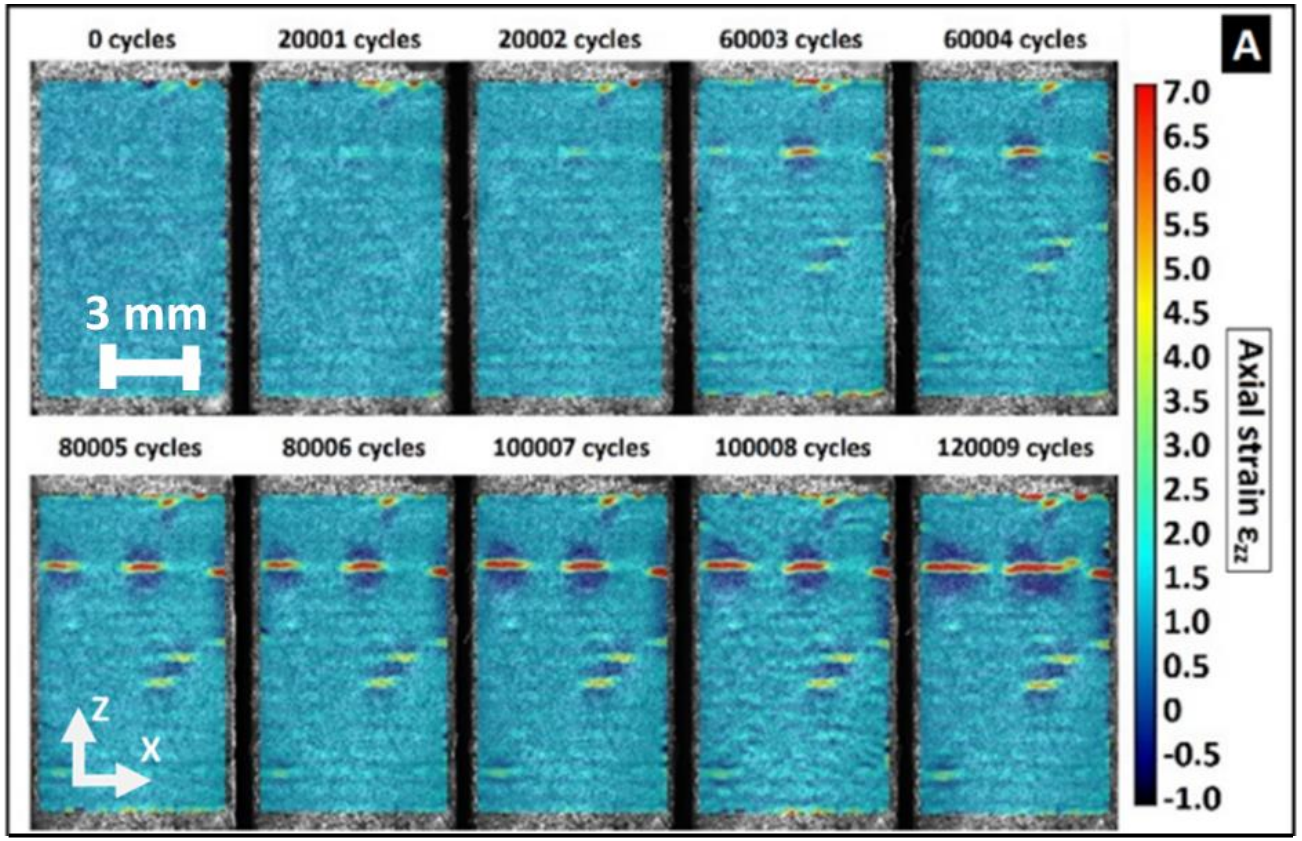

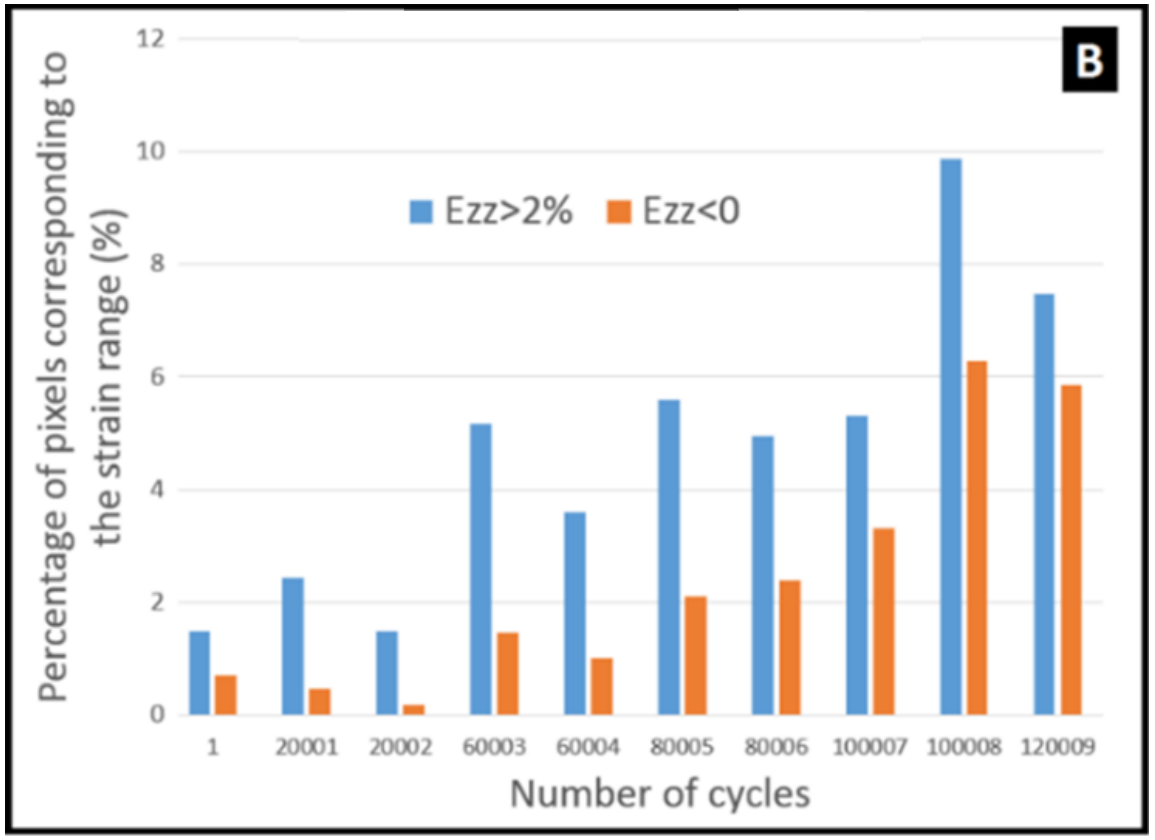

- Strain maps at max load.
- Increasing amount of extreme strains.

DIC-CT correlation

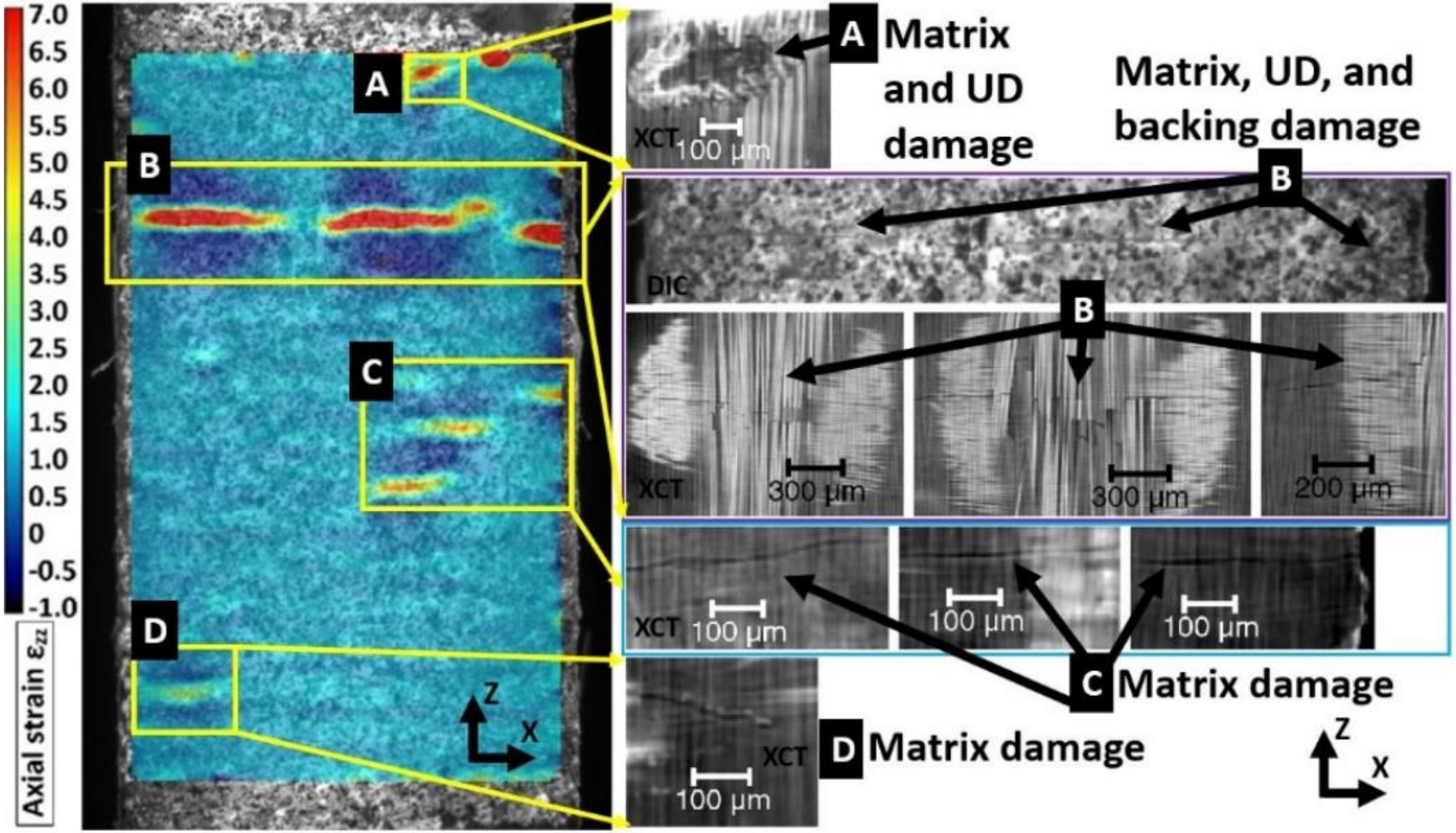

Surface damage observed in CT

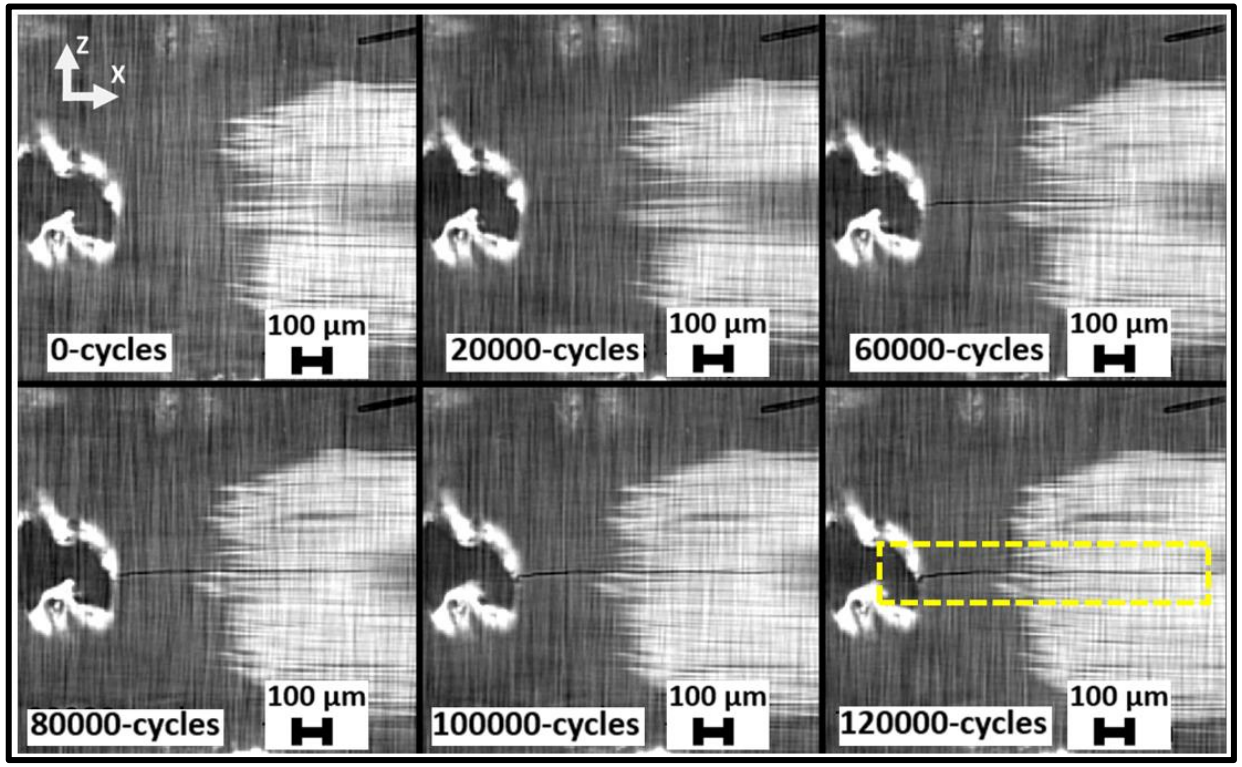

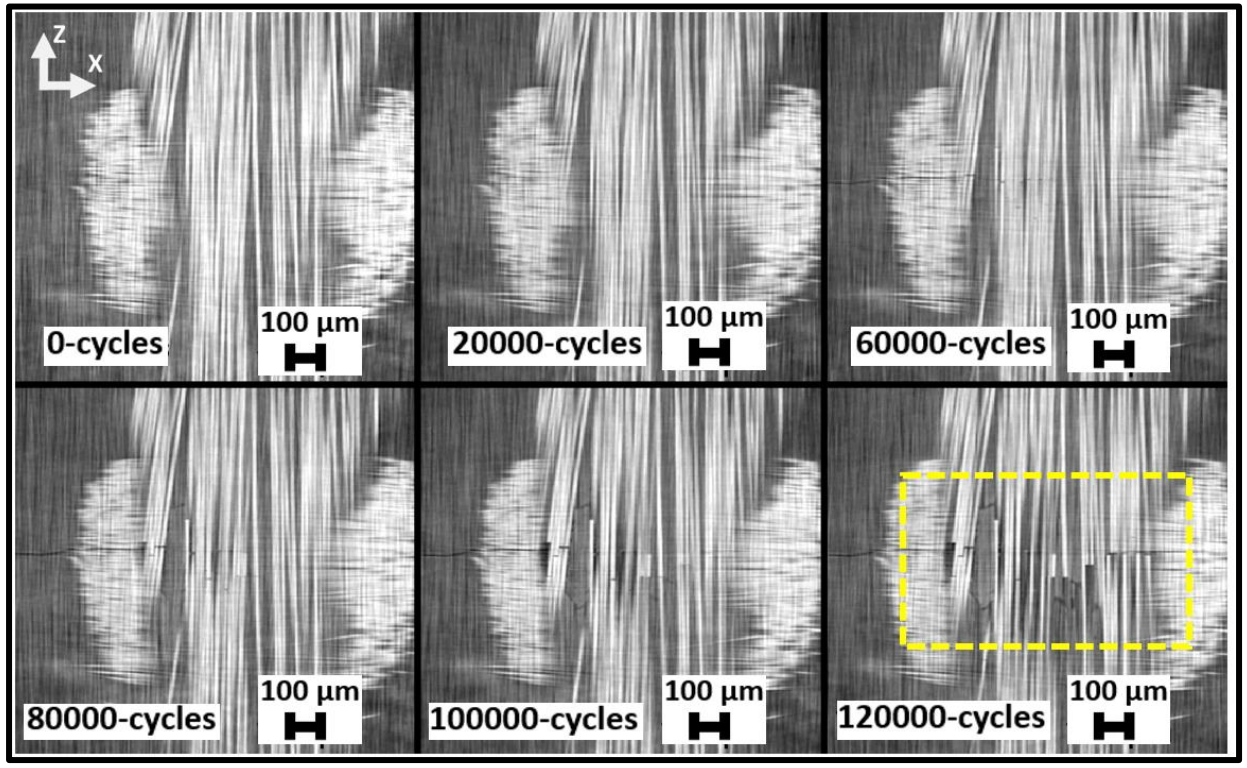

- Matrix crack originating from a surface void.
- Progresses into an off-axis crack in backing bundle.

- Off-axis crack progresses into a cluster of UD fibre breaks.

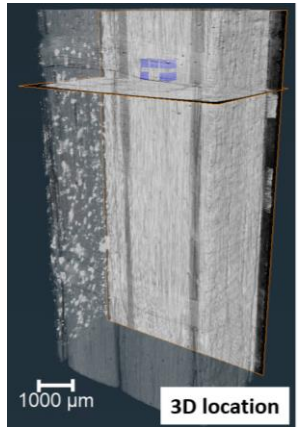

Bulk damage observed in CT

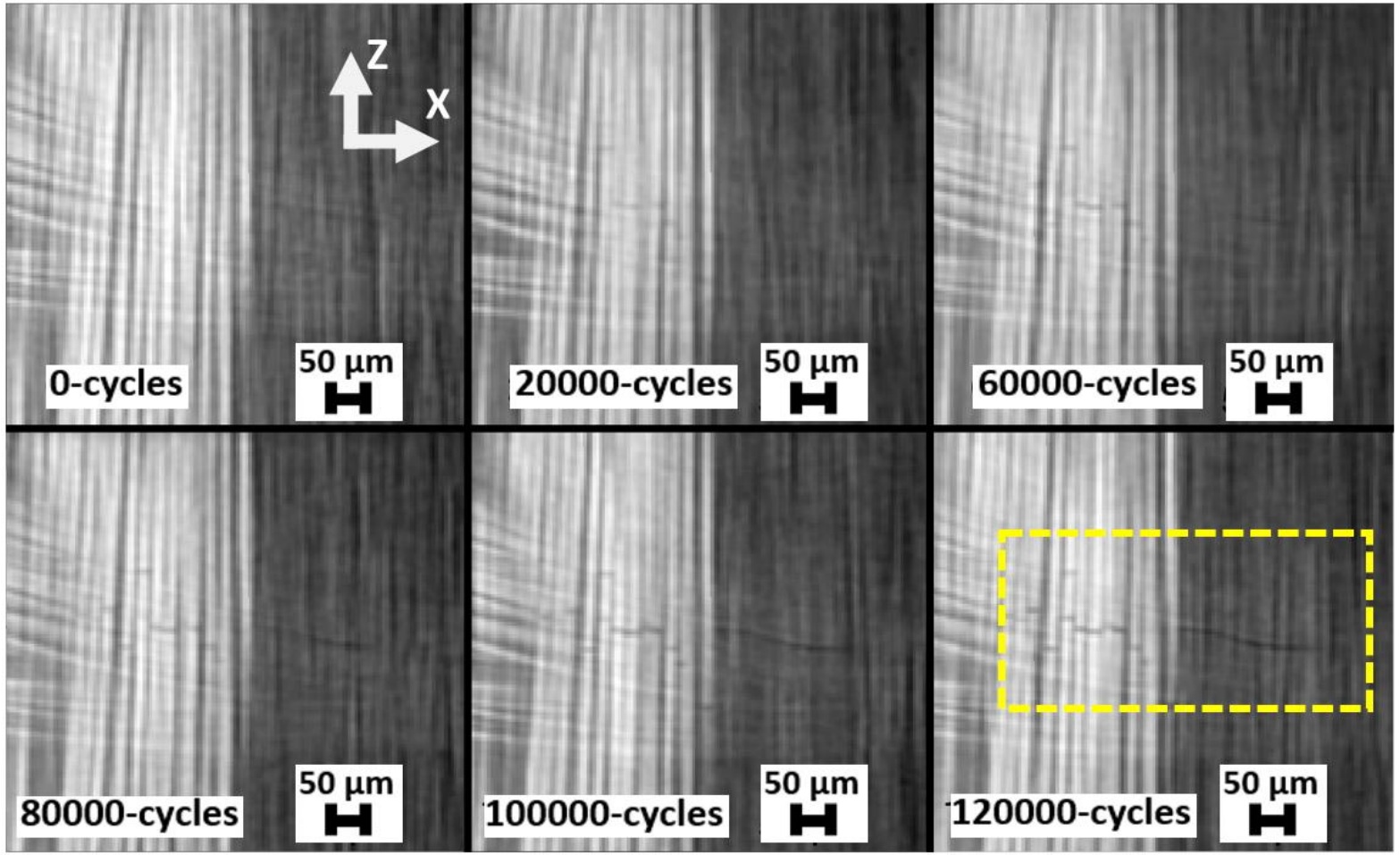

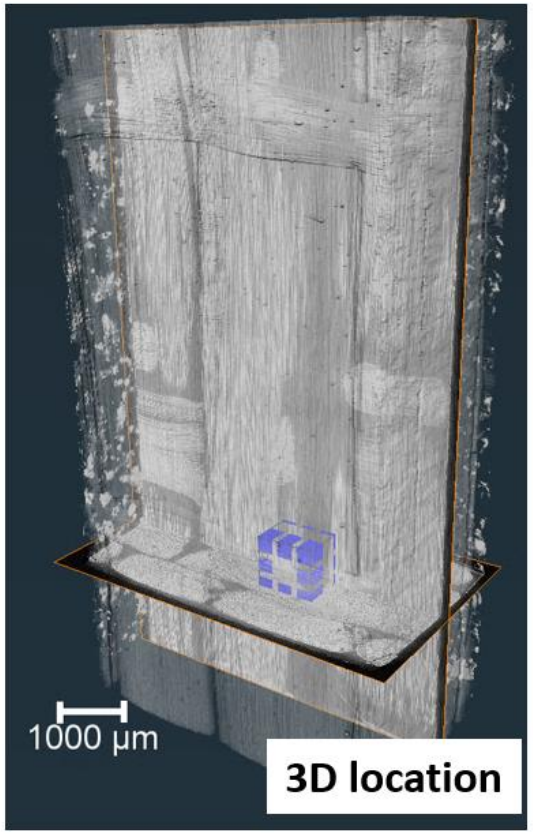

- UD fibre breaks in the bulk, close to backing bundles, give rise to localised matrix cracking.

Curved UD fibres near backing bundles in CT

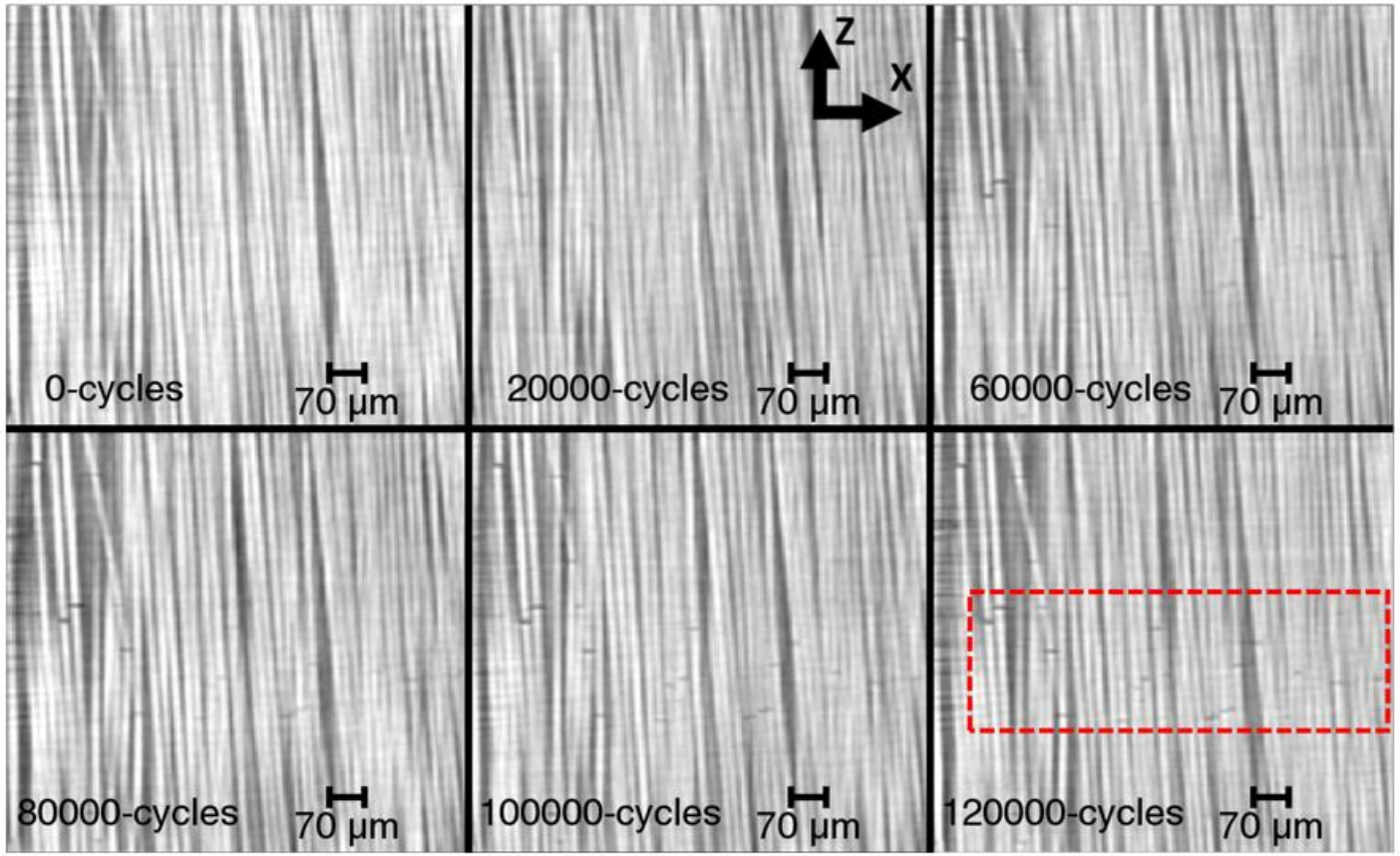

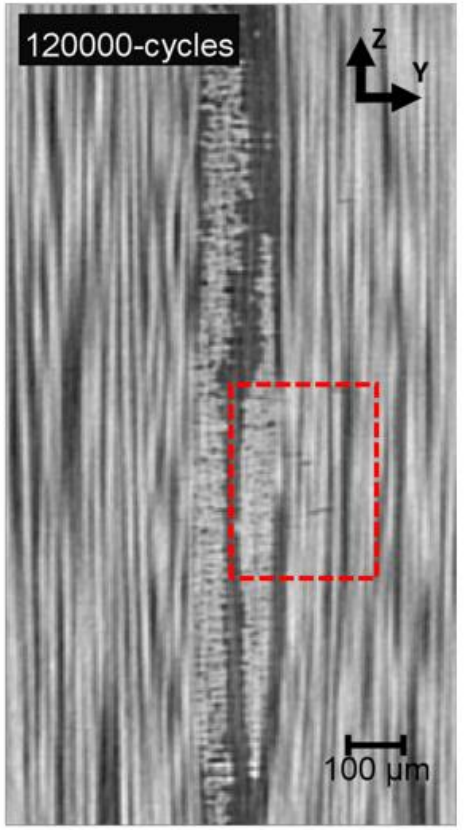

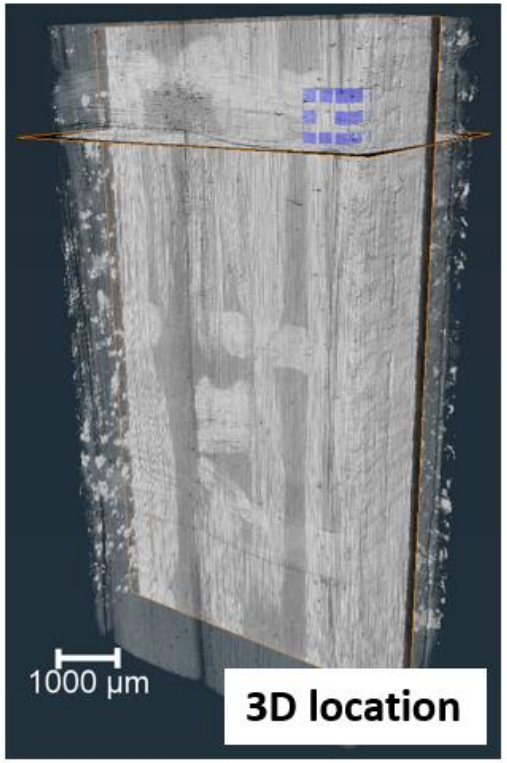

- UD fibre breaks (boxed in red) originating close to and progressing away from the backing bundles, in width.
- UD fibres appear to be straighter as they get further away from the backing bundles.

Late-stage damage observed in UD fibres CT

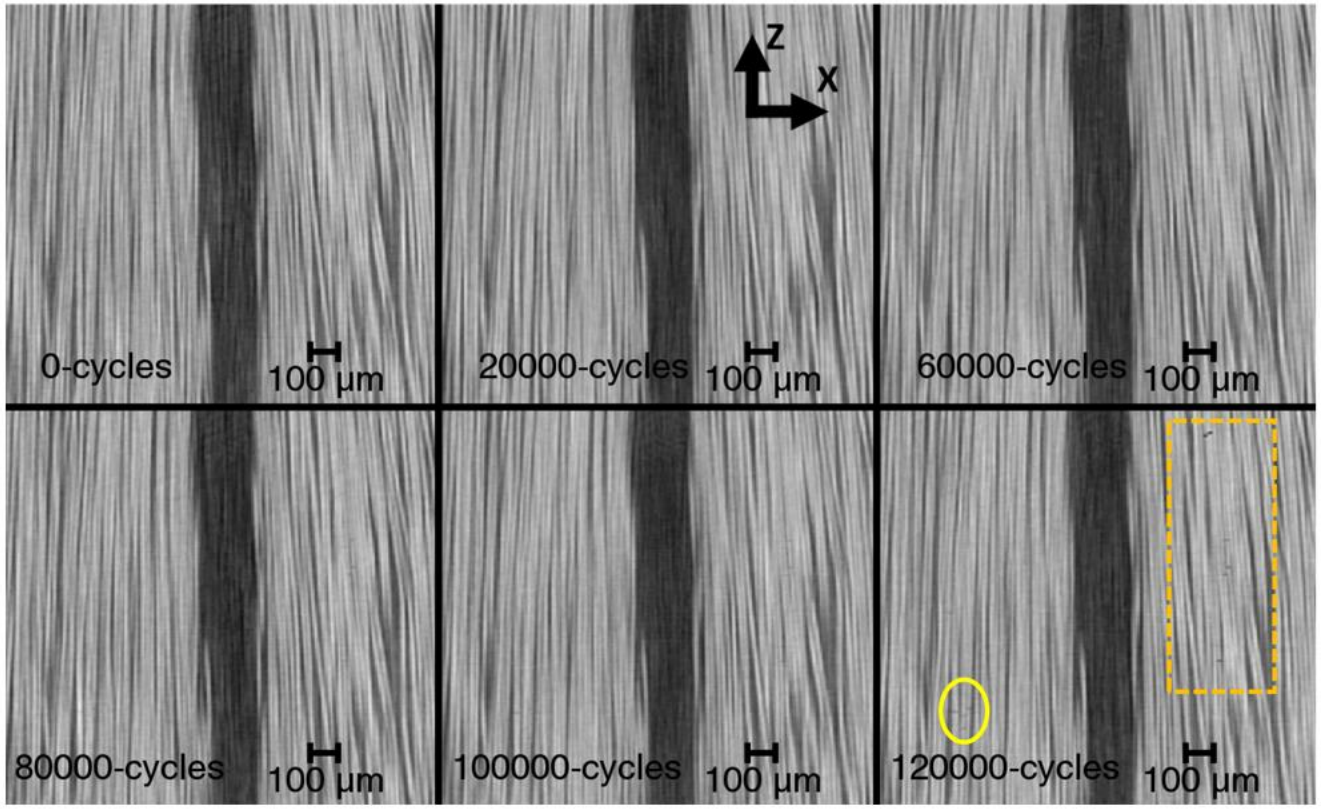

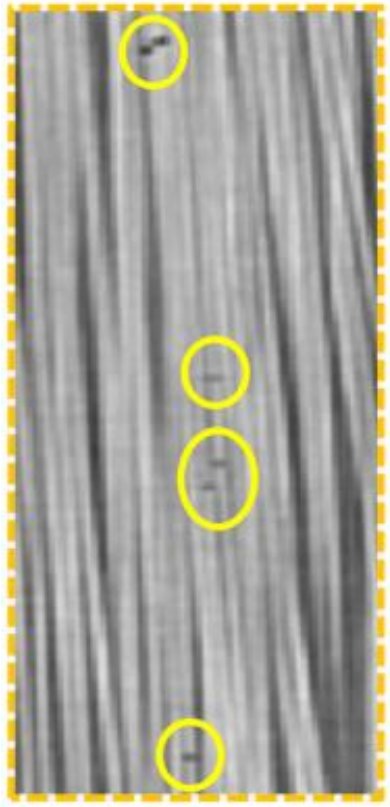

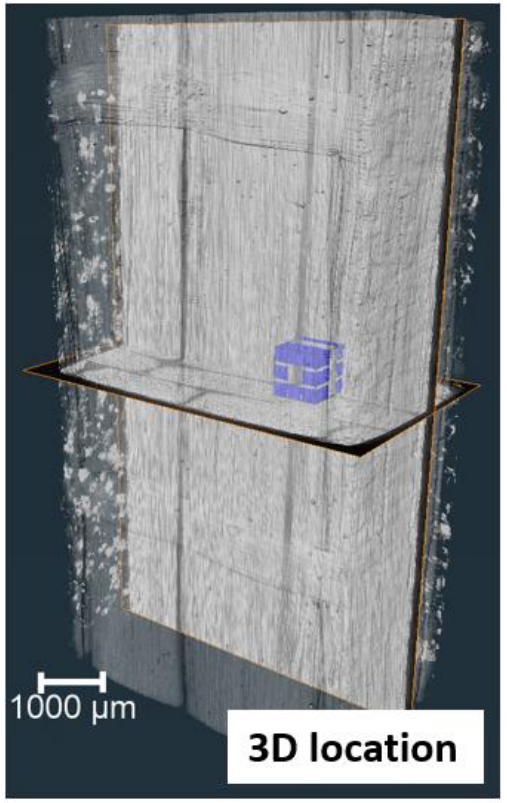

- UD fibres away from backing bundles exhibit later-stage fibre breaks, compared to the ones closer to backing bundles.

Longitudinal splits observed in CT

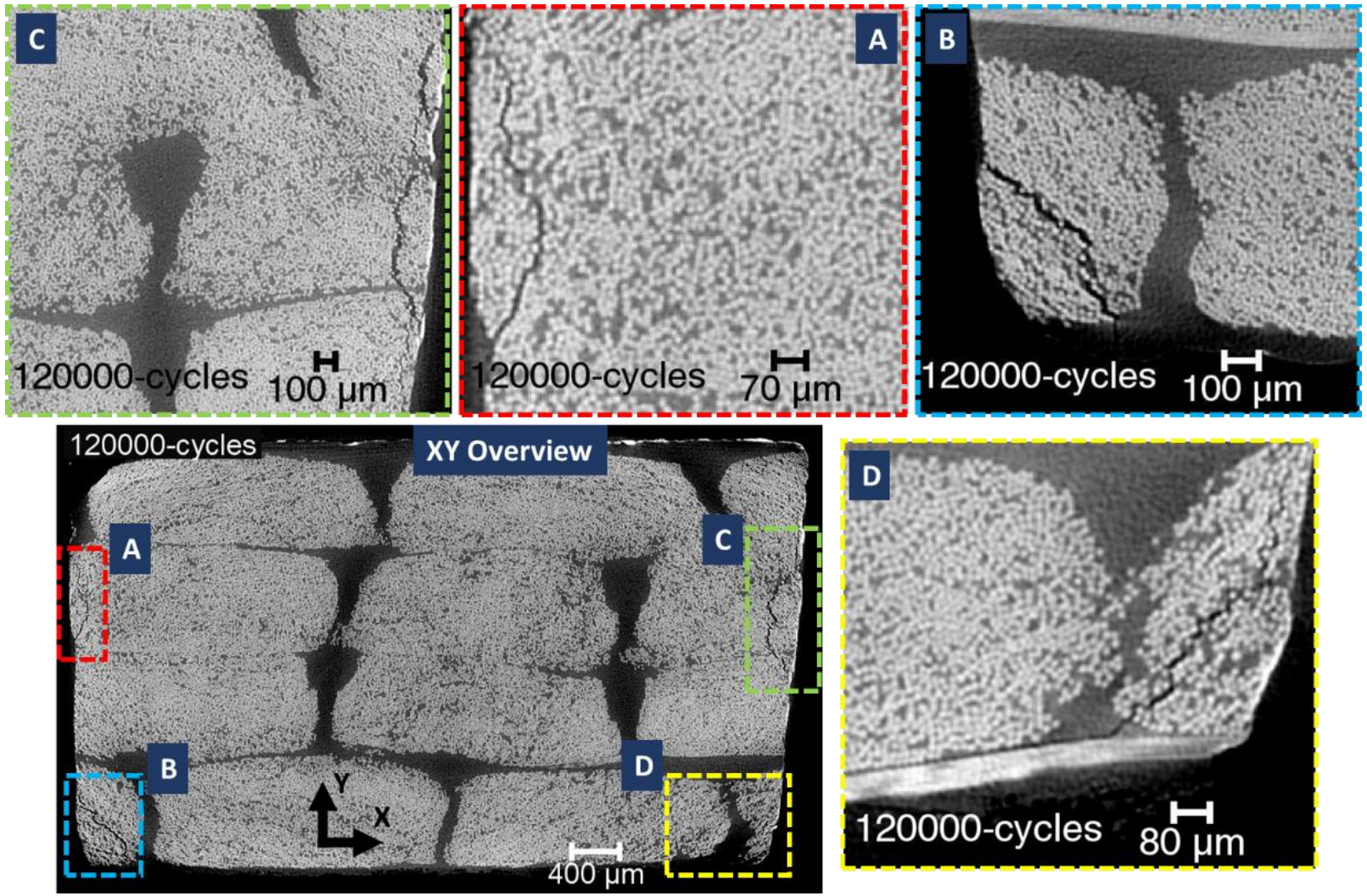

- Four longitudinal splits originating, and progressing through the length during the fatigue test.

Longitudinal split ‘D’ in CT

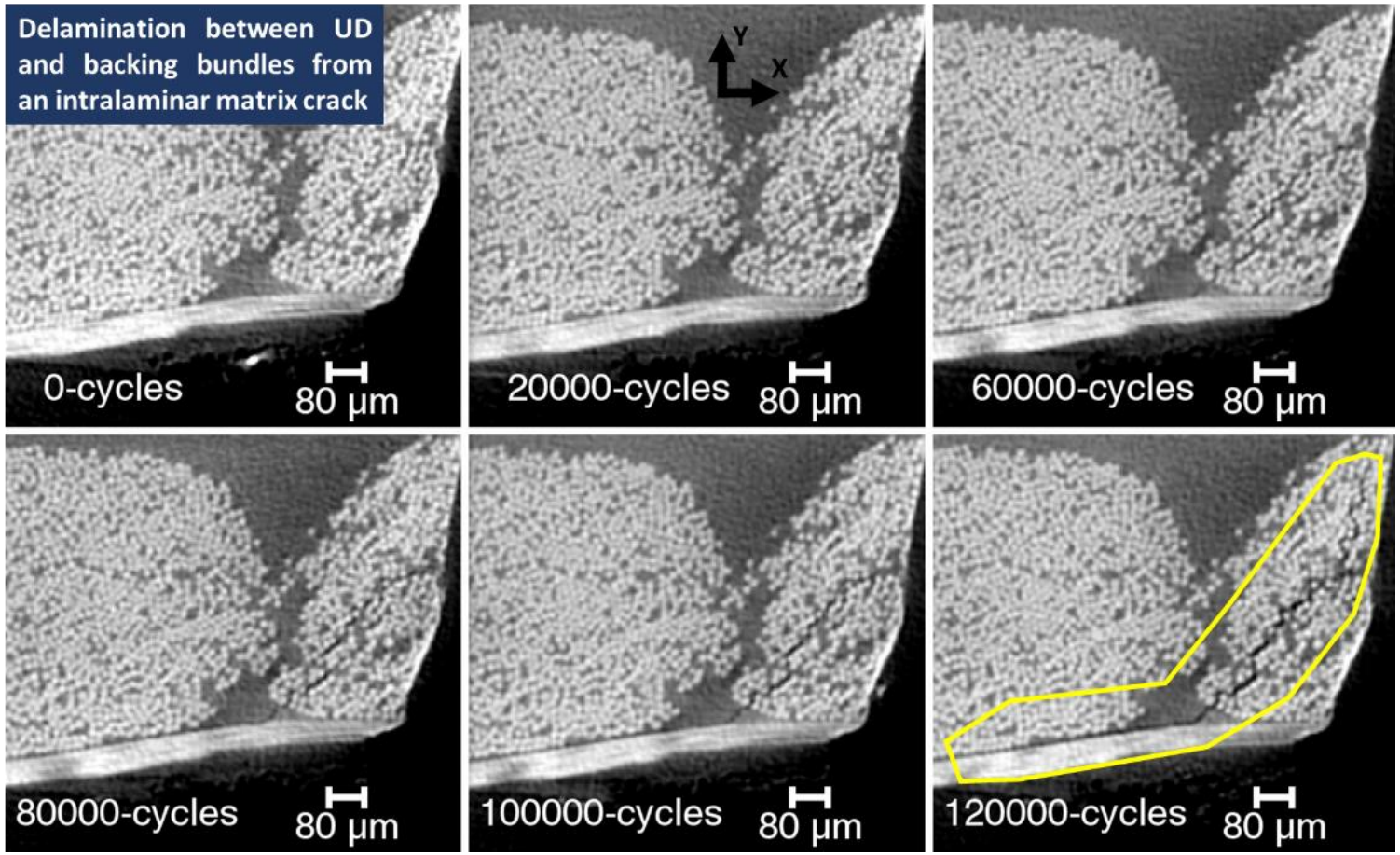

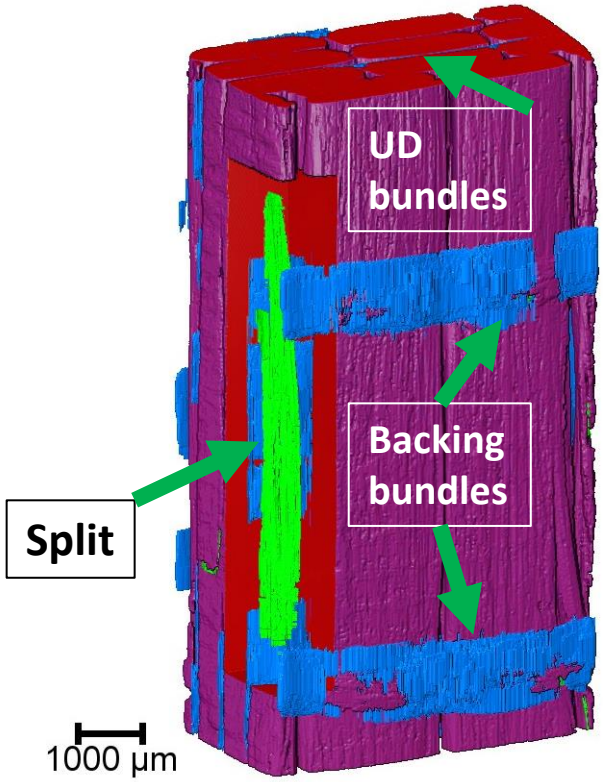

- Longitudinal split in UD bundle leading to delamination (boxed in yellow) between an adjacent UD bundle and a surface backing bundle.

Split deflection by backing bundles in CT

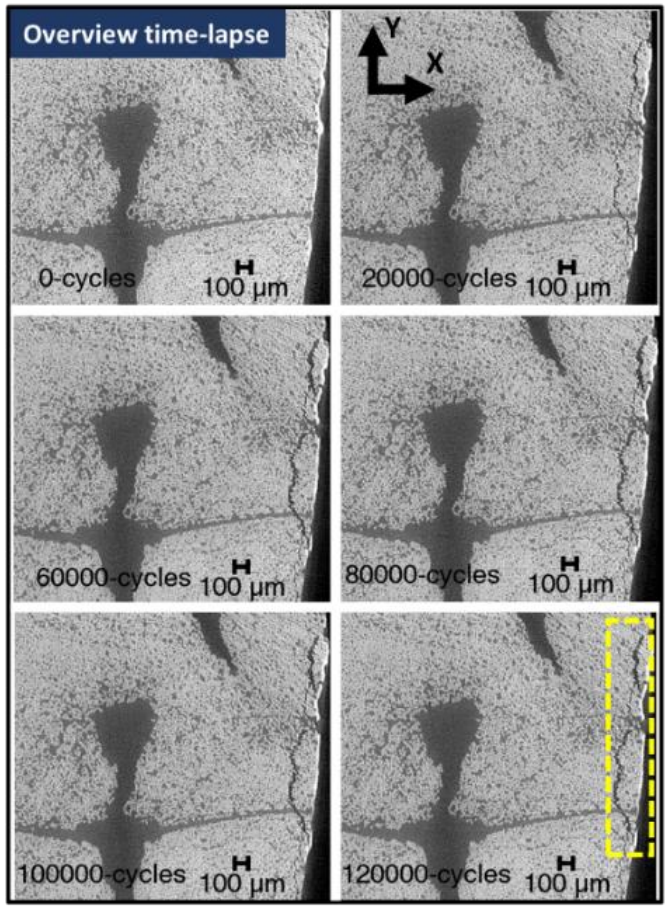

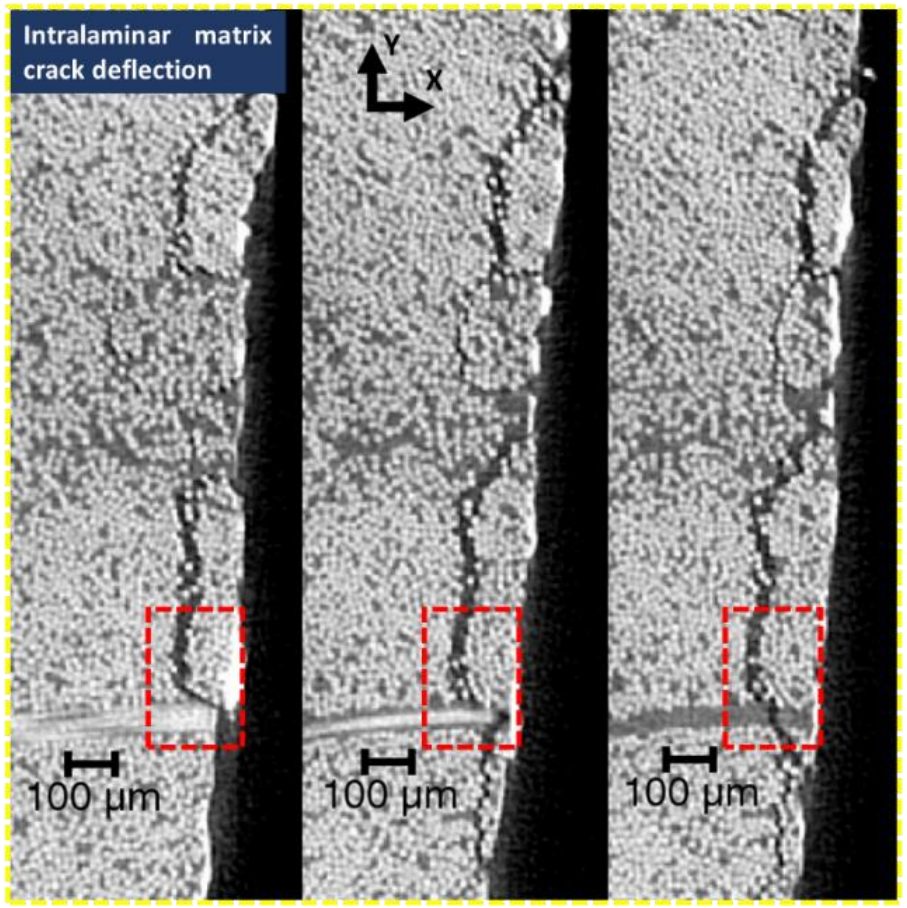

- Intralaminar split (boxed in yellow) progressing through the time-lapse, deflected by the backing bundle (boxed in red) and instead progressing around it.

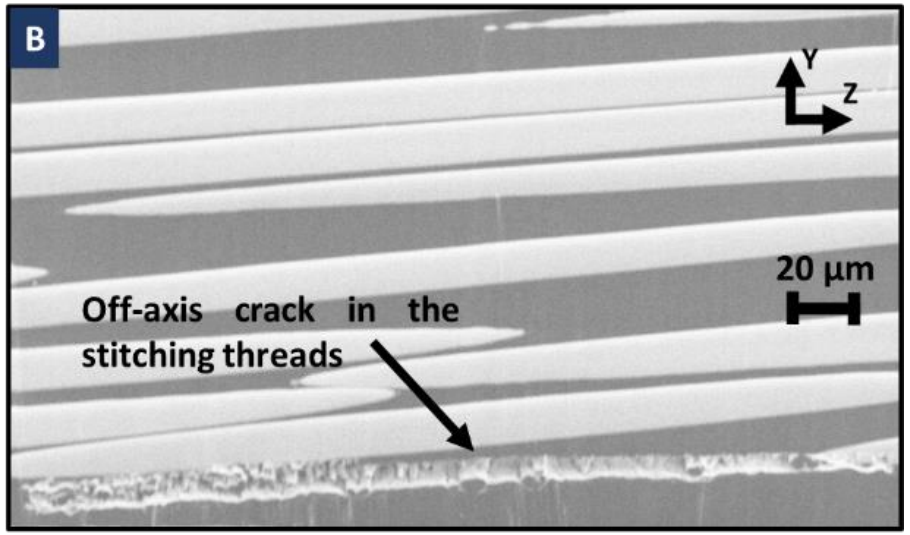

- Correlative SEM analysis points to the split deflection by the small off-axis cracks present in the stitching threads.

Agreement between damage observed in CT-Simulation-DVC

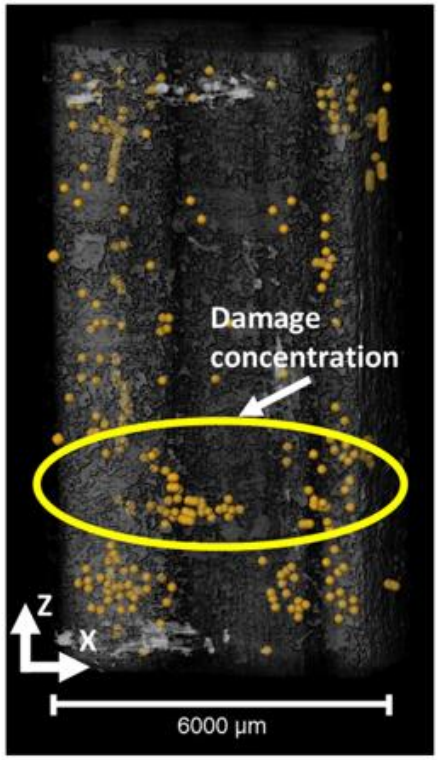

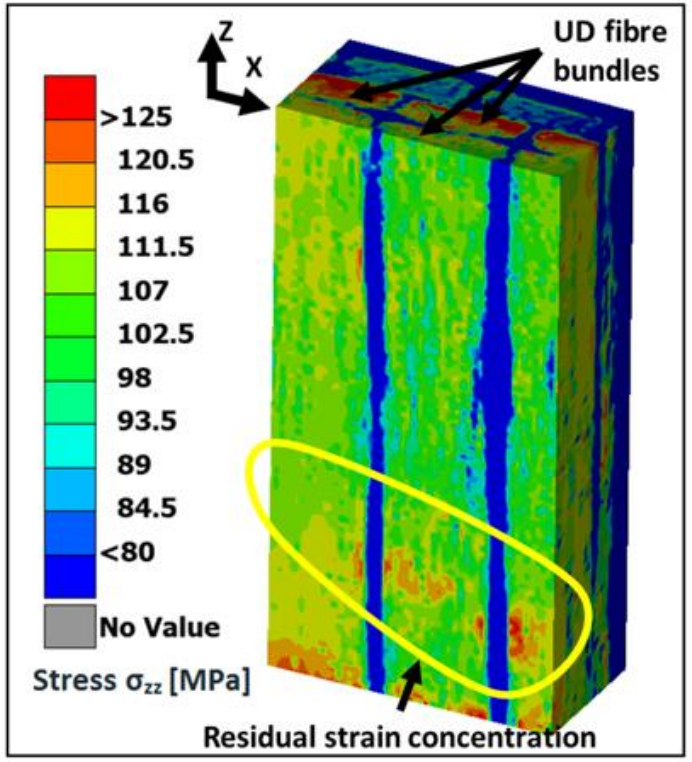

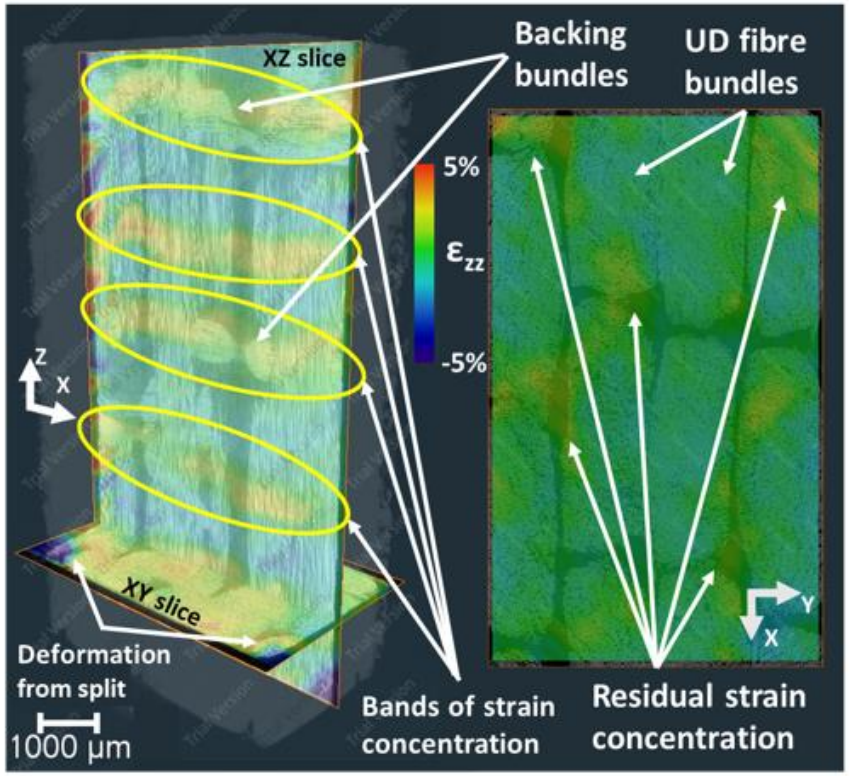

A) Damage distribution by manual observation

B) σ_{zz} obtained by tensile simulation

C) ε_{zz} obtained by DVC between 0-120k cycles

- Qualitative agreement between damage observed in CT images, predicted stress concentrations observed by tensile simulation, and strain maps obtained by DVC. In DVC, high residual strains ‘bands’ are observed in matrix-rich regions close to backing bundles. High deformation is also present near splits.

Conclusions

- Damage initiated independently on the surface and in the bulk. Voids caused matrix cracking, progressing into off-axis cracks in the backing bundles (BB). These off-axis cracks then propagated into the neighbouring UD bundles, leading to severe deformation and strain localization.

Conclusions

- Damage initiated independently on the surface and in the bulk. Voids caused matrix cracking, progressing into off-axis cracks in the backing bundles (BB). These off-axis cracks then propagated into the neighbouring UD bundles, leading to severe deformation and strain localization.
- Stronger UD fibres failure led to local compliance, leading to UD and BB fibre failures in nearby regions and a great loss in stiffness. DIC strain maps were adept at detecting and qualifying the type of damage.

Conclusions

- Damage initiated independently on the surface and in the bulk. Voids caused matrix cracking, progressing into off-axis cracks in the backing bundles (BB). These off-axis cracks then propagated into the neighbouring UD bundles, leading to severe deformation and strain localization.
- Stronger UD fibres failure led to local compliance, leading to UD and BB fibre failures in nearby regions and a great loss in stiffness. DIC strain maps were adept at detecting and qualifying the type of damage.
- Micro-notches led to micro-cracking in resin-rich regions, developing into near-surface longitudinal splits. Some of these splits got deflected/arrested by the BB and could lead to debonding of UD bundles and BB. Weka classifier in ImageJ was adept at segmenting materials phases including splits. The longitudinal morphology of the splits including their proximity to the backing bundles and the surface was exposed.

Conclusions

- Damage initiated independently on the surface and in the bulk. Voids caused matrix cracking, progressing into off-axis cracks in the backing bundles (BB). These off-axis cracks then propagated into the neighbouring UD bundles, leading to severe deformation and strain localization.
- Stronger UD fibres failure led to local compliance, leading to UD and BB fibre failures in nearby regions and a great loss in stiffness. DIC strain maps were adept at detecting and qualifying the type of damage.
- Micro-notches led to micro-cracking in resin-rich regions, developing into near-surface longitudinal splits. Some of these splits got deflected/arrested by the BB and could lead to debonding of UD bundles and BB. Weka classifier in ImageJ was adept at segmenting materials phases including splits. The longitudinal morphology of the splits including their proximity to the backing bundles and the surface was exposed.
- In the bulk, UD fibre breaks originated close to BB and proceeded more in width than in thickness due to the reduction of BB-induced waviness in width. UD fibre breaks led to matrix cracks in resin-rich regions, setting off neighbouring off-axis cracks and more UD fibre breaks. This was the mode of damage transfer within the bulk.

Conclusions

- Damage initiated independently on the surface and in the bulk. Voids caused matrix cracking, progressing into off-axis cracks in the backing bundles (BB). These off-axis cracks then propagated into the neighbouring UD bundles, leading to severe deformation and strain localization.
- Stronger UD fibres failure led to local compliance, leading to UD and BB fibre failures in nearby regions and a great loss in stiffness. DIC strain maps were adept at detecting and qualifying the type of damage.
- Micro-notches led to micro-cracking in resin-rich regions, developing into near-surface longitudinal splits. Some of these splits got deflected/arrested by the BB and could lead to debonding of UD bundles and BB. Weka classifier in ImageJ was adept at segmenting materials phases including splits. The longitudinal morphology of the splits including their proximity to the backing bundles and the surface was exposed.
- In the bulk, UD fibre breaks originated close to BB and proceeded more in width than in thickness due to the reduction of BB-induced waviness in width. UD fibre breaks led to matrix cracks in resin-rich regions, setting off neighbouring off-axis cracks and more UD fibre breaks. This was the mode of damage transfer within the bulk.
- UD fibres away from BB exhibited late-stage failure due to the absence of waviness and misalignment. From DVC results, "banding" of strain concentrations was observed across width in higher compliance regions that were resin-rich and had BB running in the same height positions.

Conclusions

- Damage initiated independently on the surface and in the bulk. Voids caused matrix cracking, progressing into off-axis cracks in the backing bundles (BB). These off-axis cracks then propagated into the neighbouring UD bundles, leading to severe deformation and strain localization.
- Stronger UD fibres failure led to local compliance, leading to UD and BB fibre failures in nearby regions and a great loss in stiffness. DIC strain maps were adept at detecting and qualifying the type of damage.
- Micro-notches led to micro-cracking in resin-rich regions, developing into near-surface longitudinal splits. Some of these splits got deflected/arrested by the BB and could lead to debonding of UD bundles and BB. Weka classifier in ImageJ was adept at segmenting materials phases including splits. The longitudinal morphology of the splits including their proximity to the backing bundles and the surface was exposed.
- In the bulk, UD fibre breaks originated close to BB and proceeded more in width than in thickness due to the reduction of BB-induced waviness in width. UD fibre breaks led to matrix cracks in resin-rich regions, setting off neighbouring off-axis cracks and more UD fibre breaks. This was the mode of damage transfer within the bulk.
- UD fibres away from BB exhibited late-stage failure due to the absence of waviness and misalignment. From DVC results, "banding" of strain concentrations was observed across width in higher compliance regions that were resin-rich and had BB running in the same height positions.
- The damaged regions in these bands and the tensile simulation that showed higher stresses in these bands point to a qualitative agreement between 3D strain maps, predicted stress and confirmed damage from XCT, corroborating the efficacy of the tensile model and the accuracy of DVC strain maps.

Conclusions

- Damage initiated independently on the surface and in the bulk. Voids caused matrix cracking, progressing into off-axis cracks in the backing bundles (BB). These off-axis cracks then propagated into the neighbouring UD bundles, leading to severe deformation and strain localization.
- Stronger UD fibres failure led to local compliance, leading to UD and BB fibre failures in nearby regions and a great loss in stiffness. DIC strain maps were adept at detecting and qualifying the type of damage.
- Micro-notches led to micro-cracking in resin-rich regions, developing into near-surface longitudinal splits. Some of these splits got deflected/arrested by the BB and could lead to debonding of UD bundles and BB. Weka classifier in ImageJ was adept at segmenting materials phases including splits. The longitudinal morphology of the splits including their proximity to the backing bundles and the surface was exposed.
- In the bulk, UD fibre breaks originated close to BB and proceeded more in width than in thickness due to the reduction of BB-induced waviness in width. UD fibre breaks led to matrix cracks in resin-rich regions, setting off neighbouring off-axis cracks and more UD fibre breaks. This was the mode of damage transfer within the bulk.
- UD fibres away from BB exhibited late-stage failure due to the absence of waviness and misalignment. From DVC results, "banding" of strain concentrations was observed across width in higher compliance regions that were resin-rich and had BB running in the same height positions.
- The damaged regions in these bands and the tensile simulation that showed higher stresses in these bands point to a qualitative agreement between 3D strain maps, predicted stress and confirmed damage from XCT, corroborating the efficacy of the tensile model and the accuracy of DVC strain maps.
- At some point, the surface and bulk damage likely joined up with larger splits to progress further and eventually lead to complete failure.

Acknowledgements

- Philip Withers, Tim Burnett (The University of Manchester)
- Ali Chirazi, Daniel Lichau (Thermo Fisher Scientific)
- Robert Auenhammer (Chalmers University of Technology)
- Lars Mikkelsen (DTU)
- Steffen Baitinger (Saertex)

Thanks to the European Training Network MUMMERING for valuable collaboration and contributions to this work.

Thanks to the European Union for financial support via grant no. 765604.